Journal of Applied Polymer Science

Crystallization and Microporous Membrane Properties of Ultrahigh Molecular Weight Polyethylene with Dibenzylidene Sorbitol

Sijun Liu, Bin Zhao, Dannong He
Functional Nanomaterial Technology Research, National Engineering Research Center for Nanotechnology, Shanghai 200240, People's Republic of China
Correspondence to: S. Liu (E-mail: sijunliu@126.com)

ABSTRACT: Dibenzylidene sorbitol (DBS) was chosen as an *in situ* forming nucleating agent to study ultrahigh molecular weight polyethylene (UHMWPE) crystallization and microporous membrane. The experimental results indicated that DBS self-assembled into fibrils first and the solution became a physical gel before UHMWPE crystallization during thermally induced phase separation (TIPS) of UHMWPE/liquid paraffin (LP)/DBS solution, and the temperature of DBS self-assembly shows a strong dependence of DBS concentration. With decreasing temperature further, DBS fibrils as heterogeneous nucleating agent accelerated UHMWPE crystallization, which was showed more clearly in UHMWPE/LP/DBS phase diagram. UHMWPE microporous membranes were prepared through TIPS method with the control of DBS concentration. It was found that UHMWPE microporous membranes in the presence of DBS fibrils show small porous size and low water permeability, but relatively larger mechanical strength. © 2014 Wiley Periodicals, Inc. J. Appl. Polym. Sci. **2014**, *131*, 40706.

KEYWORDS: membranes; self-assembly; separation techniques

Received 3 December 2013; accepted 12 March 2014
DOI: 10.1002/app.40706

INTRODUCTION

The thermally induced phase separation (TIPS) is one of the most useful techniques to prepare polymer microporous membrane and has been studied extensively for the fabrication of membrane. Generally, in the TIPS process, a homogeneous polymer and diluent blends are prepared by melt blending at a relative high temperature, then the solution is cooled to induce phase separations: liquid–liquid phase separation and solid–liquid phase separation. During liquid–liquid phase separation, a polymer-rich continuous phase and polymer-poor droplet phase or the interconnected bicontinuous structure are formed, and then grow as a result of coarsening. A cellular or a lacy structure is obtained after removing the diluent by solvent extraction, and the final membrane shows good porosity, water permeability, and higher elongation at break. Conversely, a leafy or spherulitic structure is usually obtained in the process of solid–liquid phase separation as polymer solidifies or crystallizes prior to liquid–liquid phase separation, and the resulting membrane shows excellent elastic modulus. That is to say, the different phase separation has an important influence on the final morphology and properties of microporous membrane in the TIPS process.

Ultrahigh molecular weight polyethylene (UHMWPE), as a type of engineering plastic with excellent mechanical properties and wear characteristics, has been seldom used as membrane material. One of the main reasons is probably the high viscosity and poor processability of UHMWPE. The other one is the difficulties in controlling the phase structures in UHMWPE/liquid paraffin (LP) system during TIPS. This is related to the interaction between polymer and solvent. Polyethylene has a good compatibility with LP due to their similar chemical structure and close solubility parameter ($\delta_{UHMWPE} \approx 16.12$ $J^{1/2}/cm^{3/2}$ and $\delta_{LP} \approx 15.96$ $J^{1/2}/cm^{3/2}$). Therefore, no liquid–liquid phase separation has been observed above the polyethylene crystallization in the nonisothermal process, and the control on the pore structures becomes limited solely by crystallization.[1–3] Many articles have indicated that the additive has an important effect on the structure and property of microporous membrane in the process of TIPS. For example, adding zeolite particles[4,5] to liquid–liquid thermal induced phase separation system, which complicates the droplet growth behavior and significantly influences the final cell size as the strong polymer-zeolite affinity results in the dissolved polymer migrating to the zeolite particle surface. Han et al.[6] studied the effect of different molecular weight polyethylene glycol (PEG) on pore size and porosity of polyphenylene sulfide membrane, and indicated that PEG as nucleating agent increases pore density and porosity, and decreases pore size. Cui et al.[7] prepared poly(vinylidene fluoride) (PVDF) membrane by melt blending the ternary mixture of PVDF/SiO_2/dibutyl phthalate and found that water permeability and tensile strength

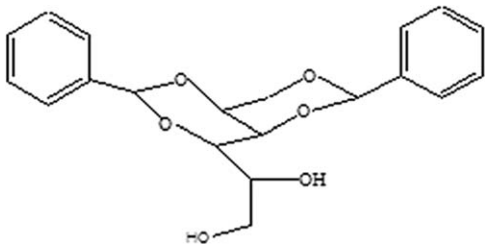

Figure 1. Chemical structure of DBS.

increase with SiO_2 content, but it reach limit content above which tensile strength do not increase due to the excessive particle disturb the formation of the spherulitic morphology in PVDF membrane. It can be inferred from all these reports that additive offers a wide route to control the porous structure and property in the process of membrane preparation.

Dibenzylidene sorbitol (DBS) is an amphiphilic molecule derived from the sugar alcohol D-glucitol. As shown in Figure 1, due to the butterfly shape and propensity to undergo intermolecular hydrogen bonding between the terminal hydroxyl group and the acetal oxygens, DBS molecules can strongly interact in the presence of an organic solvent[8,9] and form a physical gel through self-assembling into a fibril network. In fact, the self-assembly of DBS can also happen in the melt of amorphous polymer-like polystyrene or polycarbonate[10,11] and crystalline polymer such as polypropylene.[12–15] In the latter case, DBS fibrils formed from self-assembly can promote heterogeneous crystal nucleation. Many authors have indicated that DBS fibrils of 10 nm in diameter create a polymer/DBS interface as large as 400 m^2 per gram of DBS,[16,17] which assist polymer chains to crystallize into numerous small spherulites and endow the polymer with enhanced mechanical strength and optical clarity.[18,19] In our previous work,[9] we have systematically studied DBS self-assembly behavior in different solvents and clarified the effect of DBS concentration on temperature of DBS self-assembly and viscoelasticity of DBS/solvent gel. In this article, we investigate DBS self-assembly in UHMWPE/LP. The focus is about the effect of DBS fibril on UHMWPE crystallization and microporous membrane.

EXPERIMENTAL

Materials and Membrane Preparation

UHMWPE was kindly supplied by Shanghai Chemical Technology Institute, and the weight-average molecular weight is approximately 2,000,000. DBS was obtained in powder form from Miliken chemical. LP was purchased from Shanghai Chemical Reagent Factory. It is composed of short alkanes with average molecular weight of 150–250 g/mol and used without further purification.

First of all, the required quantities of DBS and LP were mixed in a glass vessel under nitrogen atmosphere at 200°C, where a clear solution was obtained. The sample was, then, cooled down to room temperature to obtain LP/DBS gel. Then, UHMWPE/LP/DBS ternary solutions were obtained by melt mixing UHMWPE and LP/DBS gel in a Batch mixer (XSS-300, Shanghai Kechang Rubber & Plastic Equipment Co, China) at 165°C for 15 min with the rotor speed 80 rpm. The concentration of UHMWPE was fixed at 10 wt %, while DBS concentration varies from 0.05 to 0.5 wt %. The homogeneous UHMWPE/LP/DBS small pieces were compressed into film (thickness ≈ 0.2 mm) under 165°C and kept for 10 min to eliminate thermal history, and subsequently cooled to room temperature with 2°C/min cooling rate. Afterward it was taken out and solidified in the liquid nitrogen. After the diluent in the sample was extracted in ethanol for 48 h and dried in vacuum oven for 24 h at 40°C, UHMWPE microporous membranes were obtained.

Rheological Measurements

The rheological measurements were performed on a rotational rheometer (Gemini 200HR, Bohlin Instruments, UK) with parallel plate geometry of 25 mm in diameter and a gap of 1.0 mm. The samples for rheological measurement were obtained by compressing UHMWPE/LP/DBS into a sheet with the thickness about 1.0 mm under 165°C and 10 MPa. Strain sweeps with strain amplitude of 0.01–1.0 at frequencies of 0.1–2 Hz were carried out to determine the linear viscoelastic range of the materials at 165°C. The annealing treatment was held at 165°C for 10 min to eliminate the pristine crystalline structures, and the stability of the sample was checked through the measurement of G′ and G″ with 0.1 Hz in the linear viscoelastic region. Little change in G′ and G″ was found over a long period (120 min) at 165°C with a strain amplitude of 1.0%, which illustrated that the effects of LP loss and thermal oxidation can be ignored.

Two rheological experiments were adopted to monitor the rheological evolution of UHMWPE/LP/DBS samples under nonisothermal and isothermal procedures. (1) Temperature ramps from 165 to 100°C for UHMWPE/LP/DBS with different DBS concentrations were carried out with 2°C/min cooling rate at a fixed frequency of 0.1 Hz and strain of 1.0%, from which the temperatures of DBS self-assembly and UHMWPE crystallization can be determined. (2) Frequency sweeps on UHMWPE/LP/DBS with varying DBS concentration at a fixed temperature 122°C were carried out to study the viscoelasticity of UHMWPE/LP/DBS gels.

Differential Scanning Calorimeter

Differential scanning calorimeter (DSC) (Q2000, TA Instruments) was adopted to study crystallization behavior in the nonisothermal process. The samples were sealed in an aluminum DSC pan, melted at 165°C and kept for 10 min to remove thermal history. Then, the samples were cooled to 40°C at different cooling rate. The onset of the exothermic peak during the cooling was taken as the nonisothermal crystallization temperature T_c. All of samples were conducted under nitrogen atmosphere.

Optical Microscopy

To study the effect of DBS fibril on UHMWPE crystallization, a small amount of the UHMWPE/LP/DBS samples were sandwiched between two glass coverslips separated by a 50-μm thick polytetrafluroethene (PTFE) spacer with a square opening in the center. The PTFE spacer allowed a uniform thickness of the sample in the observation using optical microscopy. Moreover, it could restrict LP evaporation during the experiment. The samples were heated on a hot stage (LK-600PH, Linkam, UK) at 165°C for 10 min to erase thermal history, and then, cooled

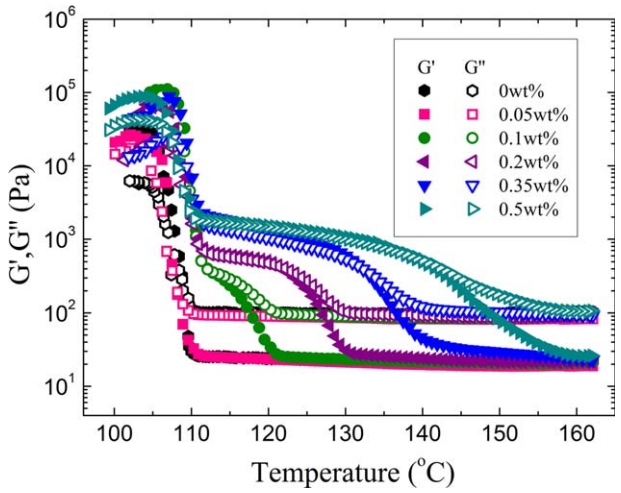

Figure 2. Temperature dependence of G′ and G″ as a function of DBS concentration at cooling rate of 2°C/min after annealing at 165°C for 10 min. [Color figure can be viewed in the online issue, which is available at wileyonlinelibrary.com.]

to room temperature at a controlled rate 2°C/min. The morphology was observed by optical microscopy (Leica DM LP, Leica Microsystems GmbH, Germany) and the images were captured using a Sony video camera.

Wide Angle X-ray Diffraction

The effect of DBS fibrils on crystalline structure of UHMWPE was studied by wide angle X-ray diffraction (WAXD) using a D/max-2200/PC Diffractometer (Rigaku Corporation, Japan) with Cu radiation. The WAXD profiles were recorded with a scanning speed of 4°/min between 5° and 45° in 2θ.

Morphological Observation

UHMWPE microporous membrane was fractured in liquid nitrogen and mounted vertically on sample holders. The surface and cross-section were sputtered with Au/Pd in vacuum, and then, examined by field emission scanning electron microscopy (JSM-7401F, JEOL, Japan) with an accelerating voltage of 5.0 KV.

Mechanical Strength

The mechanical strength of UHMWPE microporous membrane was measured with a tensile tester (Instron 4465, Instron Corp.). The membrane, punching into the dumbbell shape, was fixed vertically between two pairs of tweezers with the length of 20 mm. Then, the membrane was extended at a constant elongation rate of 100 mm/min until it was broken.

Membrane Porosity

A_k, defined as the volume of the pores divided by the total volume of the porous membrane, was applied to describe the porosity of the membrane. The dry membrane was dipped in ethanol for 24 h. Then, the membrane was taken out, and the ethanol on the surface of the membrane was softly wiped up with filter paper. Finally, the membrane was weighted quickly. The formula for A_k is as follows:

$$A_k = \frac{(\omega_0 - \omega)\overline{\rho}}{\overline{\rho}\omega_0 + (\rho - \overline{\rho})\omega} \times 100\%$$

where ω is the weight of the dry membrane, ω_0 is the weight of the wet membrane, ρ is the ethanol density, and $\overline{\rho}$ is the UHMWPE density.

Water Permeability

The water permeability of the prewet membrane by deionized water was measured through ultrafiltration cup under 0.1-MPa pressure. Time began to record after 10 min running. Then, calculated as

$$F = \frac{V}{At}$$

where F, V, A and t represent water permeability (L/m^{2}h), permeate volume (L), membrane area (m^2), and time (h), respectively.

RESULTS AND DISCUSSIONS

DBS Self-Assembly in UHMWPE/LP Solution

It is well known that DBS, as a classical thermoreversible gelator, can self-assemble into fibrils in a series of organic solvents or polymers via hydrogen bonds. The self-assembly can also happen in a solutions of solvent and polymer. Figure 2 shows the variation of G′ and G″ with temperature for UHMWPE/LP/DBS solutions containing different amount of DBS at the cooling rate of 2°C/min. In the case of low DBS concentration (0 and 0.05 wt %), G′ and G″ are seen to increase gradually when the temperature decreases down to about 110°C, where they increase abruptly. Such sudden and dramatic increase in G′ and G″ signifies the onset of UHMWPE crystallization. In contrast, G′ and G″ of sample containing 0.1 wt % DBS exhibits more complex temperature dependence. Before UHMWPE crystallization, G′ and G″ rise quickly at about 120°C, which is associated with self-assembly of DBS and the formation of DBS fibril network. With increasing DBS concentration further, the rise in G′ and G″ becomes more pronounced at higher temperature. Note that UHMWPE crystallization temperatures are increased as much as 2°C when DBS content increases, which confirms the expectation that DBS fibrils can accelerate UHMWPE crystallization through heterogeneous nucleation at temperature higher than T_c of the binary UHMWPE/LP solutions.

The transition from liquid-like state to solid-like state as DBS content increases can be seen more clearly from the frequency dependence of dynamic modulus. The dynamic modulus of UHMWPE/LP/DBS with different DBS concentrations at 122°C is shown in Figure 3. It is obvious that the samples containing 0.05 wt % DBS exhibit a homogeneous behavior according to the typical terminal property at low frequencies, $G' \sim \omega^2$ and $G'' \sim \omega$. In contrast, the significant increase in dynamic modulus can be found with samples containing 0.1 wt % DBS especially in G′ at low frequency. Moreover, the decrease in the terminal slope and the appearance of a plateau in the low-frequency region manifests the formation of certain network. As DBS concentration increases to 0.2 wt %, G′ becomes very close to G″ over wide frequencies. When the samples contain 0.35 wt % or more DBS, G′ is higher than G″ in the whole experimental frequency window, showing a pronounced elastic dominated

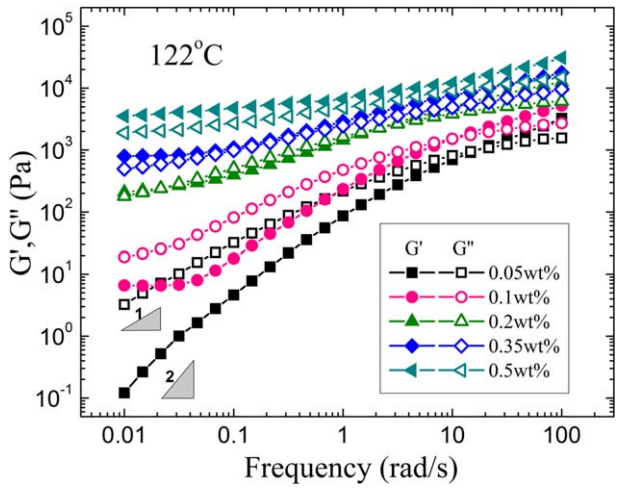

Figure 3. Frequency dependence of G′ and G″ with different DBS concentrations at 122°C and strain of 1.0%. [Color figure can be viewed in the online issue, which is available at wileyonlinelibrary.com.]

behavior. Combining the rheological features from temperature ramps and frequency sweeps, we conclude that DBS can self-assemble into fibrils which form network in UHMWPE/LP matrix with the critical DBS concentration as low as 0.1 wt %, which is similar to the self-assembly of DBS in a single solvent or polymer.

UHMWPE Crystallization in UHMWPE/LP/DBS

For UHMWPE/LP/DBS solutions containing 0.1 wt % or more DBS, the rheological results indicate that DBS molecules self-assemble into fibrils and physical gel forms before UHMWPE crystallization. It is also found that DBS fibrils can act as nucleating agent to enhance UHMWPE crystallization temperature. To elucidate UHMWPE crystallization behavior in UHMWPE/LP/DBS more clearly, the calorimetric approach DSC was adopted to estimate the effect of DBS fibrils on UHMWPE crystallization. Figure 4(a) shows the nonisothermal crystallization process of UHMWPE/LP/DBS samples containing different DBS concentrations. The onset of the exothermic peak during the cooling is taken as the crystallization temperature T_c, which is plotted as a function of DBS concentration in the inset of Figure 4(a). The obvious increase in T_c is consistent with the observation in rheological temperature ramps. T_c almost keeps a constant value when DBS amount is below 0.1 wt %. As DBS concentration increases, T_c increases at 0.1 wt % DBS. This is ascribed to the substantial increase in the number of DBS fibrils after the gel formation, which can be effective heterogeneous nucleation sites for UHMWPE molecules. Moreover, T_c shows a slight decrease at higher DBS concentration. This phenomenon can be partly interpreted as the saturation of nucleation that has been often found in the case of excessive nucleating agent[20,21] probably due to the aggregation of DBS fibrils at high DBS concentration,[9] which has also been observed by Kristiansen et al.[19] in iPP/DBS system.

Conversely, the effect of DBS fibrils on UHMWPE crystallization can also be evaluated by the half-crystallization time $t_{1/2}$. It is well known that the relative degree of crystallinity can be formulated as follows:

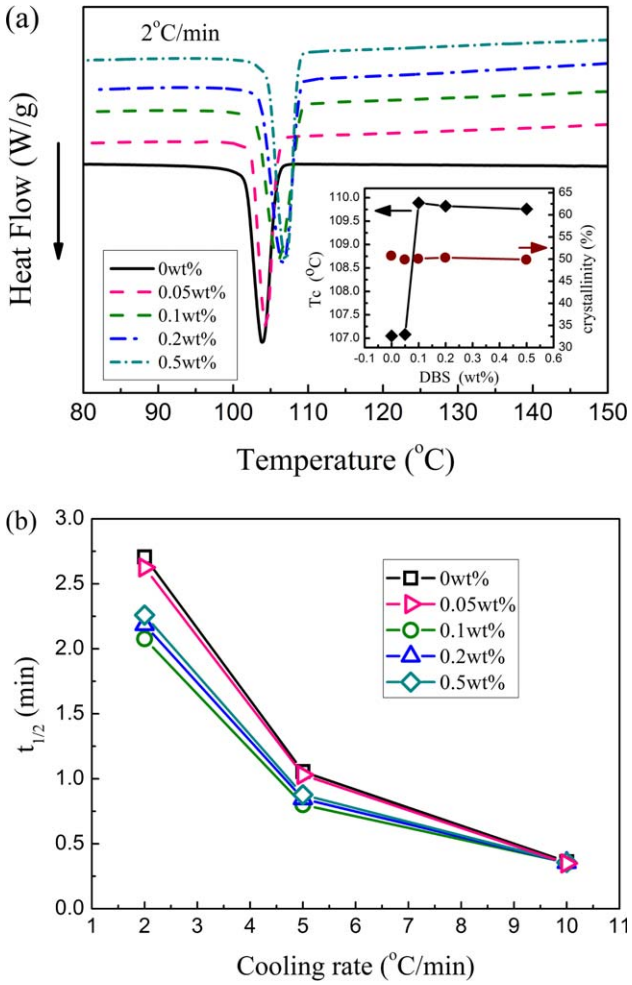

Figure 4. (a) DSC thermograms of UHMWPE/LP/DBS samples (inset: the crystallization temperature and crystallinity were plotted as a function of DBS concentration) and (b) Plot of $t_{1/2}$ versus cooling rate with different DBS concentrations in the nonisothermal process. [Color figure can be viewed in the online issue, which is available at wileyonlinelibrary.com.]

$$X(T)=\int_{T_o}^{T}\left(\frac{dH_c}{dT}\right)dT\Big/\int_{T_o}^{T_\infty}\left(\frac{dH_c}{dT}\right)dT$$

where T_o and T_∞ represent the crystallization onset and end temperatures, and dH_c is the enthalpy of crystallization released in infinitesimal temperature range dT. Horizontal temperature scale can be transformed into the time domain with the following relationship $t=(T_o-T)/v$, where T is the temperature at crystallization time t, and v is the cooling rate. $t_{1/2}$ was defined as a time to attain the degree of crystallinity 50%. It can be seen from Figure 4(b) that $t_{1/2}$ decreases with increasing cooling rates, indicating the large undercooling accelerates UHMWPE crystallization. Moreover, the heterogeneous nucleation of DBS fibrils becomes important only at low cooling rate, and the effect of DBS concentration becomes more evident at lower cooling rate. For the effect of DBS concentrations, $t_{1/2}$ decreases sharply as DBS concentration increases from 0.05 to 0.1 wt %, and then increases slightly with further increase of DBS concentration (0.2 and 0.5 wt %), which is similar to the variation of UHMWPE crystallization temperature.

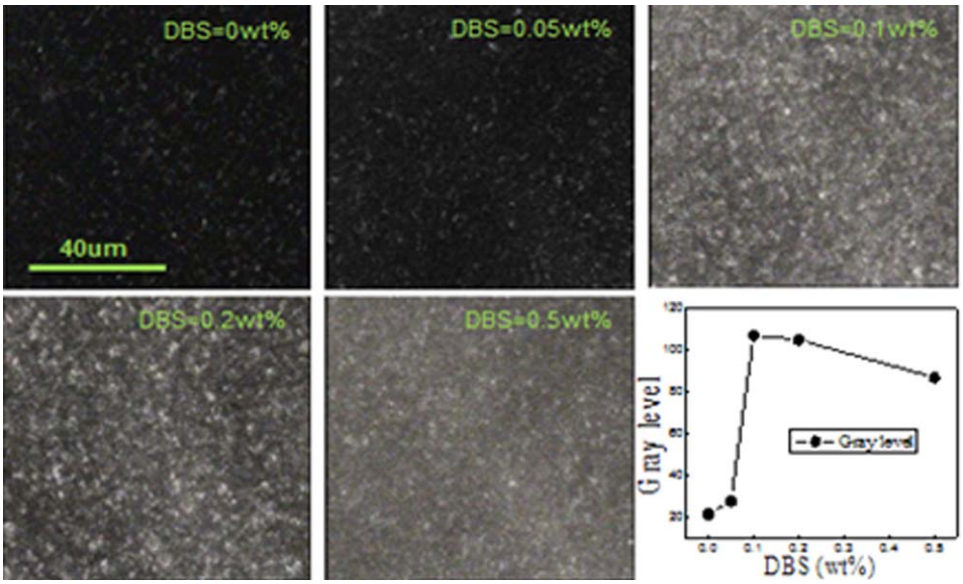

Figure 5. Polarized optical micrographs of UHMWPE/LP/DBS samples with different DBS concentrations cooled to the room temperature after annealing at 165°C for 10 min. [Color figure can be viewed in the online issue, which is available at wileyonlinelibrary.com.]

UHMWPE crystallization in UHMWPE/LP/DBS can also be viewed from POM. Figure 5 shows polarized optical micrographs for UHMWPE/LP/DBS samples containing different DBS concentrations, which undergo nonisothermal crystallization of cooling rate 2°C/min after melted at 165°C for 10 min. The photos of 0 and 0.05 wt % DBS show quite dark images. However, the great change in brightness can be seen as DBS concentration becomes higher than 0.1 wt %. The change in the brightness can be seen more quantitatively from the average gray level of POM pictures obtained by Image-Pro 6.0 software. The change in the brightness is related to the size and the density of spherulite. When the samples contain 0 and 0.05 wt % DBS, which has little effect on UHMWPE crystallization, the crystal size is larger than the light wavelength. For samples of 0.1 wt % DBS or more DBS, DBS molecules self-assemble into DBS fibrils, which as an effective heterogeneous nucleating agent enhance the nucleation density greatly. According to the definition of crystallinity, the size of crystals decreases and the number of crystals increases under the same crystallinity [the inset of Figure 4(a)]. The size of crystals becomes much smaller than the light wavelength, which causes a great increase of the brightness. With further increase of DBS concentration (0.5 wt %), however, the gray level shows a slightly decrease due to the aggregation of DBS fibrils leads to the decrease of the nucleation efficiency of DBS fibrils, which is consistent with the results of crystallization temperature and half-crystallization time.

Before further discussing the effect of DBS fibrils on UHMWPE microporous membrane, it is necessary to mention that the crystal structure of UHMWPE does not change after adding DBS. This is illustrated from the XRD results in Figure 6. It is obvious that all samples show the typical diffraction peaks of polyethylene, and the characteristic lattice planes of α crystal, that is, (110) and (200) at 21.6° and 23.9° are observed. This is different from the single-polymer system-like poly(L-lactic acid)[22] and isotactic polypropylene,[13] where DBS fibrils have an important effect on polymer crystal structure.

Phase Diagram

The apparent phase diagram of UHMWPE/LP/DBS is shown in Figure 7. T_{SA} and T_c were obtained from rheological temperature sweep as the temperature of DBS self-assembly and the temperature of UHMWPE crystallization. Both temperatures (T_{SA} and T_c) are not thermodynamic transition temperatures and are affected by the cooling rate of test. Although named as apparent transition temperatures, they are instructive on the phase behavior when the cooling rate is the same. From phase diagram, we can see three different regions corresponding to

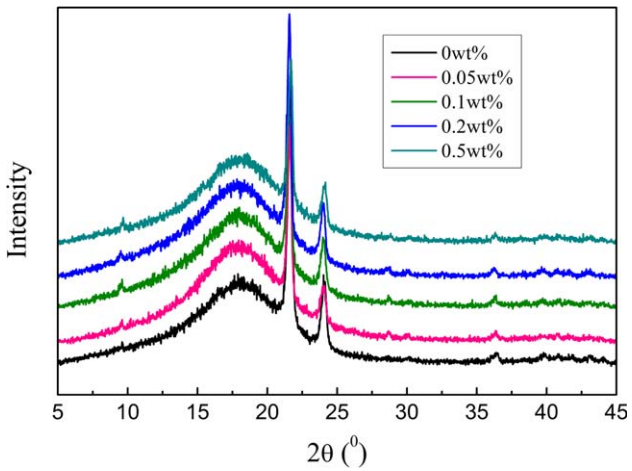

Figure 6. XRD profiles of UHMWPE/LP/DBS samples containing different DBS concentrations. [Color figure can be viewed in the online issue, which is available at wileyonlinelibrary.com.]

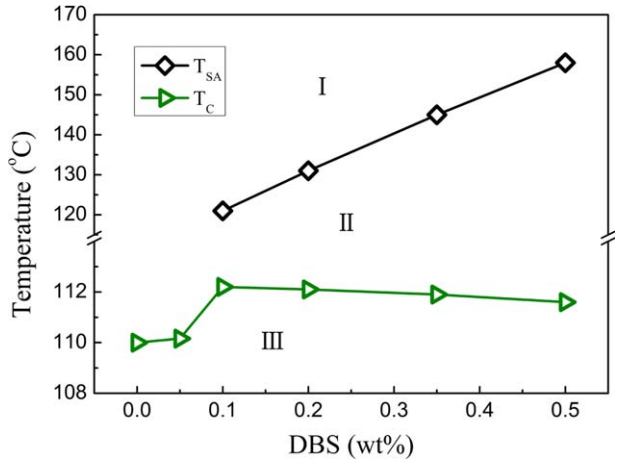

Figure 7. Phase diagram of UHMWPE/LP/DBS obtained using rheometer, T_{SA} and T_c represent the temperature of DBS self-assembly and the temperature of UHMWPE crystallization, respectively. Three regions corresponding to the three different states can be identified, Region I homogeneous solutions; Region II DBS self-assembly; and Region III UHMWPE crystallization. [Color figure can be viewed in the online issue, which is available at wileyonlinelibrary.com.]

three different physical states. In region I, UHMWPE/LP/DBS form a homogeneous solutions at high temperature. In region II, with decrease of temperature, DBS molecules self-assemble into fibrils, and UHMWPE/LP/DBS solutions become gel-like. In region III, crystallization of UHMWPE dominates. It is obvious that T_{SA} increases with increasing DBS concentration, indicating that more thermal energy is required to form gel network in a densely packed arrangement. It is seen that the effect of DBS on crystallization become obvious when its concentration is larger than 0.1 wt %. Shifting of T_c to higher temperatures denotes the acceleration of phase transitions due to the presence of DBS fibrils.

Membrane Structure and Property

Figure 8 shows the effect of DBS concentration on the structure of surface (up row) and cross-section (bottom row) of UHMWPE microporous membranes. It is apparent that all of UHMWPE membranes show a typical leafy morphology, which results typically from solid–liquid phase separation by nucleation and growth of the UHMWPE with accompanying rejection of the liquid diluent. With the increase of DBS concentration, UHMWPE microporous membranes containing the above 0.1 wt % DBS exhibit the small pore size and the uniform distribution of the pore due to DBS fibrils as nucleating agent increase the nuclei density and decrease final crystals size. Figure 9 quantitatively indicates the dependence of the average pore size on DBS concentration. The average pore size obtained as following. First, a two-color image was obtained by painting the pore black and polymer matric white via Photoshop CS5 software. Subsequently, each black domain was analyzed and the area was calculated by Scion Image software. Then, the obtained average pore size in pixels was converted into the real pore size according to the length scale. It is obvious that the average radius decreases to 0.4 μm approximately in the presence of DBS fibrils, which already meet the size requirement of microfiltration membrane in water treatment. Moreover, with the increase of DBS concentration further, the pore size has a slight increase due to the decrease of the nucleation efficiency of the aggregated DBS fibrils.

Figure 10 shows the stress-strain curves of UHMWPE microporous membranes. It is obvious that the stress and strain increase sharply during DBS concentration is higher than 0.1 wt %, which indicates that adding a certain amount of DBS improves the mechanical strength of UHMWPE microporous membrane. This result is different with polymer microporous membrane added by inorganic fillers. Cui et al.[7] studied PVDF membrane modified by SiO_2, and the experimental results indicated that the tensile strength and elongation at break initially increase with the addition of SiO_2 and reach a peak when SiO_2 concentration were 2 wt %, and then, decline as SiO_2 concentration was further increases due to the affinity between PVDF and untreated SiO_2 is small which leads to an excessive amount inorganic SiO_2 had a negative effect on PVDF tensile strength. Many articles[23,24] also showed that the pore sizes have an

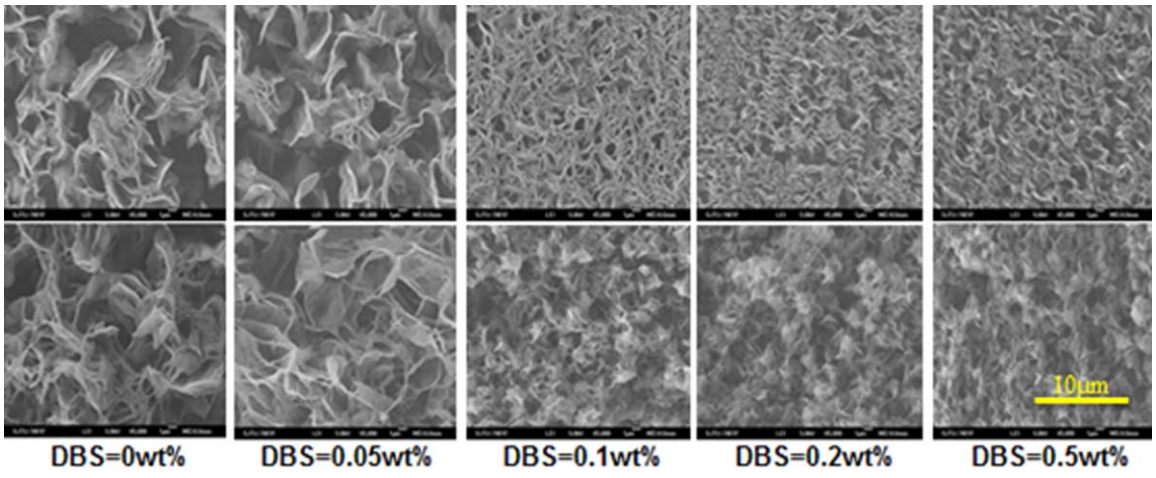

Figure 8. Effect of the different DBS concentration on the structure of UHMWPE microporous membrane (up: surface; bottom: cross-section). [Color figure can be viewed in the online issue, which is available at wileyonlinelibrary.com.]

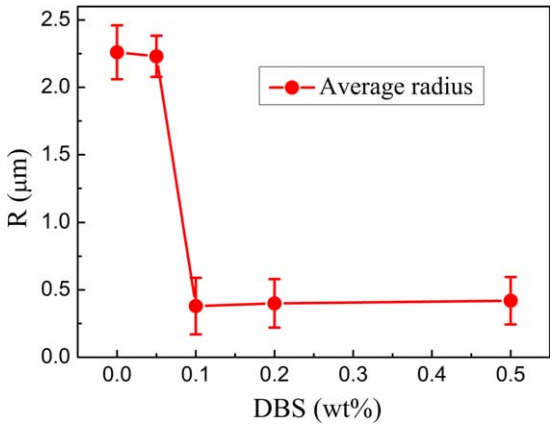

Figure 9. The dependence of the pore sizes of UHMWPE microporous membrane on DBS concentration. [Color figure can be viewed in the online issue, which is available at wileyonlinelibrary.com.]

important influence on the tensile strength and elongation at break. The macroporous sizes usually lead to a weak tensile strength and low elongation at break because the macroporous structure is more easily deformed. However, for UHMWPE microporous membrane obtained using *in situ* formed DBS fibrils as nucleation agent, the increase of mechanical strength of UHMWPE microporous membrane could be, conversely, ascribed to the denser porous structure. Conversely, the presence of dense DBS fibril network serves as a template for the packing of UHMWPE spherulites, which can also lead to the increase of mechanical strength.

The effect of DBS concentration on the water flux and porosity of UHMWPE microporous membrane is shown in Figure 11. It is obvious that the porosity is almost independent of DBS concentration, which is consistent with the reports[25,26] that the porosity is usually determined by the diluent volume fraction in the polymer/diluent mixture. This implies that although the nucleation density increases in the presence of DBS fibrils, the extent of solid–liquid phase separation between UHMWPE and

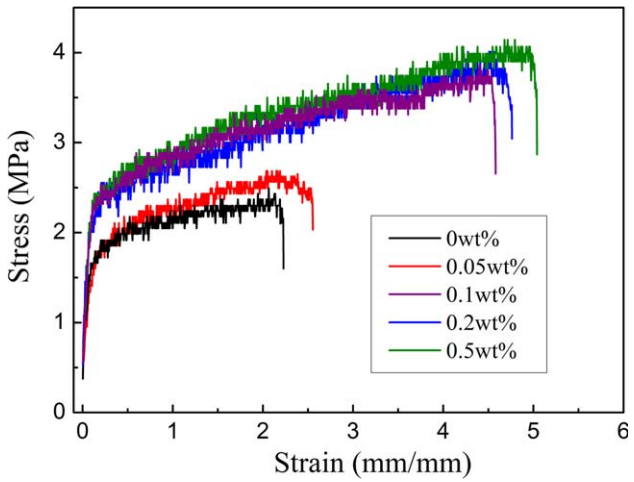

Figure 10. The dependence of mechanical strength of UHMWPE microporous membrane on DBS concentration. [Color figure can be viewed in the online issue, which is available at wileyonlinelibrary.com.]

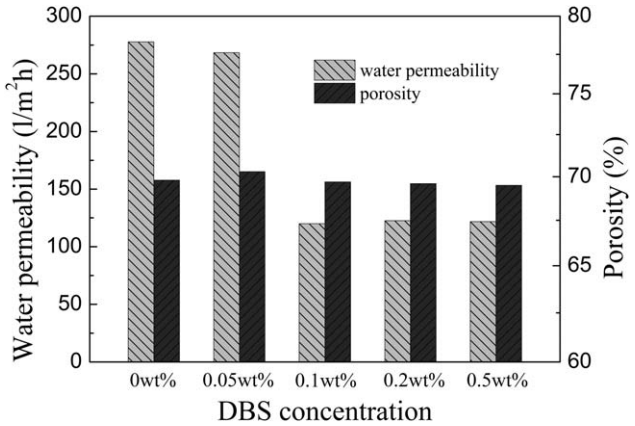

Figure 11. The dependence of water permeability and porosity of UHMWPE microporous membrane on DBS concentration.

LP are not affected. Moreover, the water permeability decreases as DBS concentration increases. This is because that the pathway of water across the membrane increases greatly in small pores, which makes the water permeability decrease.

CONCLUSIONS

In this article, we studied DBS self-assembly in UHMWPE/LP and the effect of DBS fibrils on UHMWPE crystallization and the structure and properties of UHMWPE microporous membrane. The experimental results indicated that DBS self-assembles into fibrils first and the blends exhibit a gel state with decreasing temperature, and the temperature of DBS self-assembly shows a strong dependence of DBS concentration. DBS fibrils formed after self-assembly of DBS can act as effective heterogeneous nucleating agent rise the temperature of UHMWPE crystallization and accelerate the rate of UHMWPE crystallization. UHMWPE membrane was prepared by TIPS method. It has been found that the pore size and water permeability greatly decrease due to the increase of the nuclei density and the pathway of water molecules across the membrane. However, the mechanical strength remarkably increases in the presence of DBS fibrils because of the denser DBS fibrils network and the small porous structure.

ACKNOWLEDGMENTS

The authors gratefully acknowledge the project supported by the National High Technology Research and Development Plan of China (also called 863 Plan; Grant No. 2013AA031801), the Foundation Research Project of Shanghai Science and Technology Commission (Grant No. 13NM1401600), and International Science and Technology Cooperation Project of China, contract grant number (Grant No. KY201302007).

REFERENCES

1. Sun, H.; Rhee, K. B.; Kitano, T.; Mah, S. I. *J. Appl. Polym. Sci.* **1999**, *73*, 2135.

2. Matsuyama, H.; Okafuji, H.; Maki, T.; Teramoto, M.; Kubota, N. *J. Membr. Sci.* **2003**, *223*, 119.

3. Shen, L.; Peng, M.; Qiao, F.; Zhang, J. L. *Chin. J. Polym. Sci.* (English Edition) **2008**, *26*, 653.
4. Funk, C. V.; Lloyd, D. R. *J. Membr. Sci.* **2008**, *313*, 224.
5. Funk, C. V.; Beavers, B. L.; Lloyd, D. R. *J. Membr. Sci.* **2008**, *325*, 1.
6. Han, X.; Ding, H.; Wang, L.; Xiao, C. *J. Appl. Polym. Sci.* **2008**, *107*, 2475.
7. Cui, A.; Liu, Z.; Xiao, C.; Zhang, Y. *J. Membr. Sci.* **2010**, *360*, 259.
8. Chen, W.; Yang, Y.; Lee, C. H.; Shen, A. Q. *Langmuir* **2008**, *24*, 10432.
9. Liu, S.; Yu, W.; Zhou, C. *Soft Matter* **2013**, *9*, 864.
10. Mitra, D.; Misra, A. *Polymer* **1988**, *29*, 1990.
11. Lai, W. C.; Tseng, S. J.; Chao, Y. S. *Langmuir* **2011**, *27*, 12630.
12. Balzano, L.; Portale, G.; Peters, G. W. M.; Rastogi, S. *Macromolecules* **2008**, *41*, 5350.
13. Balzano, L.; Rastogi, S.; Peters, G. W. M. *Macromolecules* **2008**, *41*, 399.
14. Sreenivas, K.; Basargekar, R.; Kumaraswamy, G. *Macromolecules* **2011**, *44*, 2358.
15. Sreenivas, K.; Pol, H. V.; Kumaraswamy, G. *Polym. Eng. Sci.* **2011**, *51*, 2013.
16. Thierry, A.; Fillon, B.; Straupé, C.; Lotz, B.; Wittmann, J. C. *Prog. Colloid Polym. Sci.* **1992**, *87*, 28.
17. Thierry, A.; Straupe, C.; Wittmann, J. C.; Lotz, B. *Macromol. Symp.* **2006**, *241*, 103.
18. Kristiansen, M.; Tervoort, T.; Smith, P.; Goossens, H. *Macromolecules* **2005**, *38*, 10461.
19. Kristiansen, M.; Werner, M.; Tervoort, T.; Smith, P.; Blomenhofer, M.; Schmidt, H. W. *Macromolecules* **2003**, *36*, 5150.
20. Nogales, A.; Mitchell, G. R. R.; Vaughan, A. S. *Macromolecules* **2003**, *36*, 4898.
21. Seo, M. K.; Lee, J. R.; Park, S. J. *Mater. Sci. Eng. A* **2005**, *404*, 79.
22. Lai, W. C. *Soft Matter* **2011**, *7*, 3844.
23. Lin, Y.; Tang, Y.; Ma, H.; Yang, J.; Tian, Y.; Ma, W.; Wang, X. *J. Appl. Polym. Sci.* **2009**, *114*, 1523.
24. Qiu, Y. R.; Matsuyama, H.; Gao, G. Y.; Ou, Y. W.; Miao, C. *J. Membr. Sci.* **2009**, *338*, 128.
25. Zhou, H.; Wilkes, G. L. *J. Mater. Sci.* **1998**, *33*, 287.
26. Lu, X.; Li, X. *J. Appl. Polym. Sci.* **2009**, *114*, 1213.